Estuarine, Coastal and Shelf Science 218 (2019) 59–69

Contents lists available at ScienceDirect

Estuarine, Coastal and Shelf Science

journal homepage: www.elsevier.com/locate/ecss

Assessment of phytoplankton photosynthetic efficiency based on measurement of fluorescence parameters and radiocarbon uptake in the Kara Sea

Sergey A. Mosharov[a,b,*], Valentina M. Sergeeva[a], Vyacheslav V. Kremenetskiy[a], Andrey F. Sazhin[a], Svetlana V. Stepanova[a]

[a] Shirshov Institute of Oceanology, Russian Academy of Sciences, Moscow, 117997, Russia
[b] Bauman Moscow State Technical University, Moscow, 105005, Russia

ARTICLE INFO

Keywords:
Chlorophyll fluorescence
Relative electron transport rate
Primary production
Diatoms
Shelf
Kara Sea

ABSTRACT

Spatial distribution of relative electron transport rate (rETR) values, the maximum quantum efficiency of PSII (F_v/F_m), and biomass-specific primary production (P^B, mg C (mg Chl *a*)$^{-1}$ h^{-1}) were described for the eastern part of the Kara Sea in the autumn (September). A characteristic feature of this period was a noticeable decrease in the length of the day and the elevation angle of the sun, leading to a significant decrease in surface photosynthetically active radiation (PAR). Despite low light in the euphotic zone, the phytoplankton maximum quantum efficiency of PSII (F_v/F_m) was high (0.5–0.7) in the upper 30-m layer of the water column, which indicates a potentially active state of phytoplankton. At the same time, the main productive activity of phytoplankton was linked to the surface 0–3 m and was closely related to the daily incident PAR and the share of diatoms in the total phytoplankton biomass. Despite a decrease in light level and following a reduction in the values for productive characteristics of the phytoplankton community, diatoms continued to play a major role in primary productivity in the eastern Kara Sea at the end of the vegetative season. Comparative analysis of data obtained by two different techniques – fluorescence measurements and experimental carbon fixation estimations – demonstrated a close relationship between rETR and P^B. However, surface values of P^B changed more strongly than rETR, which may, apparently, reflect different efficiency in the use of absorbed light energy in the synthesis processes. Photosynthetic efficiency, reflecting the extent of use of the light energy caught in processes of organic matter synthesis, can be expressed through the ratio between P^B and rETR values. The P^B/rETR ratio increased in areas characterized by drastic gradients of hydrophysical conditions: over the external coastal shelf, central shelf and lower continental slope of the St Anna Trough.

1. Introduction

Primary production in the Arctic seas is strongly influenced by the annual light regime, with long dark winters allowing very little or no photosynthesis. As a result, Arctic marine primary productivity is very highly seasonal (Alexander, 1995). Short-term rates of primary production are light-limited during spring because of ice (Glud et al., 2007; Mosharov et al., 2018). Vertical stratification has been highlighted as a key controlling factor of the productivity and structure of marine ecosystems of the Arctic Ocean (Carmack, 2007). During the autumn, at the end of a growth season, photosynthetically active radiation (PAR) becomes the main factor for primary productivity (Platt et al., 1987; Hegseth, 1997; Brugel et al., 2009; Yun et al., 2012), corresponding with low solar radiation in polar regions in this season.

Investigations of chlorophyll fluorescence parameters and phytoplankton primary production were carried out in two latitude sections in the Kara Sea in autumn. For a variety of biotopical conditions, the Kara Sea is a unique basin. It is defined by complicated mechanisms of interaction among waters of various origin. On the one hand, surface water over the eastern continental shelf of the Kara Sea is constantly freshened by enormous runoff from the largest Siberian Rivers – Ob and Yenisei – during the growth season (Kubryakov et al., 2016). At the same time, formation of surface-freshened lenses, the distribution of which depends on wind velocity and direction, is possible all over the shelf (Zatsepin et al., 2010a). On the other hand, to the north, in the slope and deep-water areas there are interactions among Kara Sea shelf

* Corresponding author. Nahimovskiy Prospect, 36, Moscow, 117997, Russia.
E-mail address: mosharov@ocean.ru (S.A. Mosharov).

https://doi.org/10.1016/j.ecss.2018.12.004
Received 20 September 2018; Received in revised form 3 December 2018; Accepted 5 December 2018
Available online 06 December 2018
0272-7714/

water, Arctic waters and transformed Atlantic water (Zatsepin et al., 2015). In addition, the Yamal Current propagates along the 100-m isobaths, spreading Barents Sea water to the Kara Sea shelf (Zatsepin et al., 2010b).

In the frame of the long-term Kara Sea ecosystem studies organized by SIO RAS over the continental shelf, in the St Anna Trough, and in the Ob and Yenisei Rivers estuaries in 2007–2017, the spatial variability of phytoplankton structure, distribution of chlorophyll *a*, and primary production during the autumn period have been described in detail (Mosharov, 2010; Sukhanova et al., 2010, 2015a; Demidov et al., 2014, 2015b; Mosharov et al., 2016; Sergeeva et al., 2016).

At present, the modern research methods of phytoplankton communities based on measurement of active chlorophyll fluorescence parameters are under increasing interest. These parameters characterize the concentration of chlorophyll *a* in algae populations, their potential photosynthetic activity, the relative rate of electron transport utilized via photochemistry, and the quantum efficiency of photosynthesis (Krause and Weis, 1991). The fluorescence method, in comparison with standard research techniques for the state and functioning of phytoplankton, allows acquisition of more information with a higher accuracy without requiring special sample preparation for a shorter period. For the last 30 years, a fluorescence method for assessment of the physiological state of phytoplankton (Bergmann et al., 2002; Alderkamp et al., 2012) and their photosynthetic ability (Barranguet and Kromkamp, 2000; Schreiber, 2004), including a balance between carbon fixation and other electron consuming pathways (Badger et al., 2000; Beardall et al., 2001; Bukhov and Carpentier, 2004), has been widely used in the world practice of ecological studies due to intensive development and improvement of instruments which have become more sensitive and mobile (Röttgers, 2007; Erga et al., 2014).

The maximum quantum efficiency of photosynthesis (F_v/F_m) is often used as an indicator of nutrient stress (Sakshaug et al., 1997; Kolber et al., 1990; Falkowski and Raven, 2007), functional state and physiological changes in phytoplankton (Suggett et al., 2009b; Aldercamp et al., 2012; Garrido et al., 2013; Erga et al., 2014), as well to estimate photoadaptation and photoinhibition (Alderkamp et al., 2011) in toxicological studies on the impact of various substances on the photosynthetic apparatus of different plankton algae types (Matorin et al., 2009).

Traditionally, primary production has been measured chemically. One approach is to measure rates of photosynthetic oxygen evolution, such as in the light and dark bottle method (Strickland and Parsons, 1972). Another common technique uses radioactive ^{14}C as a tracer (Steemann-Nielsen, 1952). A common disadvantage shared by the oxygen and ^{14}C uptake methods is that they require that the samples be incubated in a container, creating artifacts. Another important limitation of both techniques is that the required incubations are time-consuming, and this limits the practical sampling rate.

The fluorescence method of measuring primary production is based on using multicomponent models including the maximum fluorescence (F_m), the initial fluorescence when all reaction centres are open (F_0), the reoxidation rate of Q_a (τ_q), and the functional absorption cross-section of photosystem II (PSII) (σ_{PSII}), as well as the initial fluorescence (F') and maximum fluorescence (F_m') under ambient light (Suggett et al., 2010; Lawrenz et al., 2013). One of the key components of these models is the relative electron transport rate (rETR), calculated on the basis of fluorescence parameters for light-acclimated samples (F' and F_m'). Carbon fixation does not take place in PSII; however, a fraction of the electrons passed from PSII to photosystem I (PSI) is used for this purpose. Estimates of carbon fixation rates measured using the ^{14}C uptake method (primary production) are commonly compared with those derived from variable fluorescence.

The relationship between ETR and C fixation/O_2 production has been compared in a range of studies on algal cultures and pelagic ecosystems; generally, linear correlations are documented between ETR and gross C fixation and/or O_2 production (Kromkamp et al., 2008; Suggett et al., 2009a; Hancke et al., 2015). In some studies, the interrelations between ETR and C fixation have also been shown to be species-specific (Suggett et al., 2009a). Lately, studies have been directed towards deriving the electron requirement for photosynthesis. Variability of the electron requirement and photosynthetic efficiency has been discussed (Hancke et al., 2015). Lawrenz et al. (2013) compiled a large amount of ETR data obtained using FRRF (fast repetition rate fluorescence) instruments and compared them to available ^{14}C uptake rates across different regions.

In a situation where relative changes rather than absolute values will suffice, the equation for calculating ETR can be simplified, and rETR values are used. The rETR parameter is frequently used as a measure of photosynthetic rate (Ralph et al., 2002; Morris and Kromkamp, 2003). Measurement of the rETR value is a fast and simple procedure, with determination of a minimal set of fluorescence parameters. The value of rETR allows a quantitative estimate of the rate of solar energy transition to chemical energy, providing biosynthesis of organic substances in phytoplankton cells. The fluorescence method (determination of rETR) can estimate photosynthetic potential whereas the radiocarbon method (determination of chlorophyll-specific carbon fixation rate, P^B) is an approximate measure of the actual rate of photosynthesis (Öquist et al., 1982). Photosynthetic performance, reflecting the extent of use of the light energy caught in processes of organic matter synthesis, can be expressed through the ratio between rETR and P^B values.

Thus, the rETR value is a convenient parameter for assessment of the variability of phytoplankton photosynthetic performance with changing environmental conditions. It should be noted that using chlorophyll fluorescence (in particular, rETR) to estimate the photosynthetic rate and physiological state of phytoplankton is characterized by both advantages (non-intrusive character, rapid assessment, non-incubation) and problems. More recently, Suggett et al. (2009b) have shown strong species-specific characteristics of variable fluorescence parameters (mostly F_v/F_m and σ_{PSII}) and warned against a strictly physiological interpretation of these parameters at sea. The quantum yield of chlorophyll *a* fluorescence in vivo is highly variable due to a variety of environmental cues that dictate the physiological responses and lead to changes in photochemical and non-photochemical quenching.

Research into the spatio-temporal variability of these parameters in natural populations of phytoplankton is very interesting not only in terms of studying the physiological response of phytoplankton to changes in the hydrological parameters of the water column or anthropogenic influence but also as an assessment of the potential efficiency of food resources for higher links of a trophic chain in different regions of the World Ocean during various seasons.

Polar marine regions are characterized by a short growth season because of the regional peculiarity of light regimes which are determined by ice cover during most years and by low annual solar radiation. These conditions determine the photosynthetic potential of Arctic phytoplankton. Spring conditions are the most favourable for phytoplankton production. However, determination of potential food resources for higher trophic levels requires an estimate of the primary production for the growth period as a whole. Estimating the efficiency of solar energy assimilation by phytoplankton and use of it for organic matter synthesis (primary production) is an actual task.

The aim of this work is to study the spatial variability of phytoplankton fluorescence parameters characterizing photosynthetic activity, such as the maximum quantum efficiency of PSII and rETR as well as the interaction between these parameters and carbon assimilation, and environmental factors in the eastern Kara Sea in autumn.

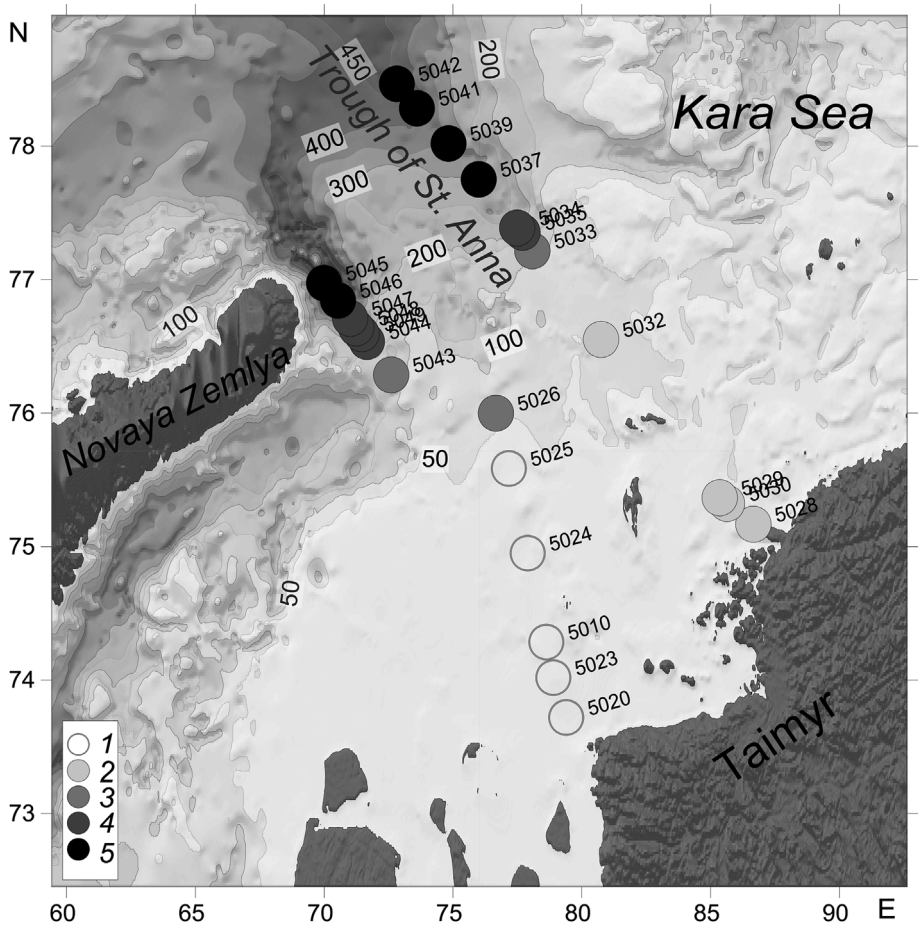

Fig. 1. Research area and station locations: *1, 2* – coastal zones, *3* –continental central shelf, *4* –shelf edge, *5* –St Anna Trough's continental slope.

2. Material and methods

2.1. Research area and sampling procedure

Materials for the study were collected during the 59th cruise of R/V *Akademic Mstislav Keldysh* (from 17 September to 29 September 2011) in the Kara Sea at 24 stations at 73° 43′–78° 28′ N and 69° 59′–86° 39′ E. The research was carried out in the Yenisei River estuary and over the continental slope (St. 5020–5026), and in the St Anna Trough both in the eastern branch (St. 5032–5042) and in the central branch (St. 5043–5049) (Fig. 1).

Water samples were collected from eight depths within the 120-m surface layer using Niskin bottles settled on a 'Rozette' equipped with a CTD (SBE-19 Plus; Sea Bird Equipment, USA). Sampling depths were chosen as a result of CTD casts down as well fluorescent profiling obtained by the SBE-19 Plus equipped with sensors for measuring fluorescence and turbidity.

The water samples were divided into subsamples, which were used for measurement of different parameters like nutrient and chlorophyll concentrations, experimental carbon fixation estimations (primary production), chlorophyll fluorescence, and abundance and biomass of phytoplankton.

2.2. Nutrient analysis

Fixation of dissolved oxygen and NH_4 in the samples was performed directly after sampling. Samples to determine pH, nutrients (silicates, phosphates and nitrogen forms) and alkalinity were selected in 0.5-l plastic bottles without preservation and were treated immediately after sampling. For work in the areas with a considerable quantity of POM (bays and river–sea interfaces), the water samples were preliminarily filtered through a 1 μm Nuclepore filter. The dissolved inorganic phosphorous ($P\text{-}PO_4$), dissolved inorganic silicon ($Si(OH_4)$), nitrite nitrogen ($N\text{-}NO_2$), nitrate nitrogen ($N\text{-}NO_3$) and ammonium nitrogen ($N\text{-}NH_4$) concentrations were measured by using standard procedures (Grasshoff et al., 1999).

2.3. Measurement of primary production, chlorophyll a and surface irradiance

Primary production was measured onboard using the ^{14}C uptake method (Steemann-Nielsen, 1952) at 24 stations in the study region. Water samples were collected at eight optical depths (100%, 79%, 64%, 49%, 24%, 6%, 3% and 2% of downwelling PAR above the sea surface). The samples were incubated for 3 h in an ICES photosynthetron (HydroBios, Germany) with circulating water from a HAILEA H-100 aquarium chiller (China) to keep ambient surface temperature (which varied from 2.9 to 5.7 °C for different stations). The samples were exposed to eight appropriate light levels, which were achieved with neutral density filters (PAR irradiance values of 300, 237, 192, 147, 72, 18, 9 and 6 μmol photons $m^{-2} s^{-1}$). After incubation, flasks were filtered onto a 0.45-μm 'Vladipore' membrane (Russia). Radioactivity of the samples was determined using a Triathler (Hidex, Finland) liquid scintillation counter.

Biomass-specific PP, P^B (mg C (mg chlorophyll $a)^{-1}$ day^{-1}) was calculated by normalizing PP at different depths to the corresponding chlorophyll *a* (Chl *a*) concentration.

Chl *a* concentration was measured fluorometrically (JGOFS, 1994). Seawater samples (500 ml) were filtered onto Whatman GF/F (glass-fibre filters) under a low vacuum (~0.3 atm). For extraction, Chl *a* filters were placed in acetone (90%) and maintained at temperature of

+4 °C in the darkness for 24 h. Then fluorescence of the extracts was measured with a Turner Designs fluorometer (Trilogy Fluorometer) before and after acidification with 1 N HCl. The fluorometer was calibrated before and after each cruise using pure Chl *a* (Sigma) as a standard. The concentration of Chl *a* and phaeophytin a was calculated according to Holm-Hansen and Riemann (1978).

At all sampling events, surface PAR (400–700 nm) was measured with a Li-Cor Li-190 Quantum Sensor, and underwater irradiance with a Li-Cor Li-193 Underwater Quantum Sensor, both attached to a Li-Cor Li-1400 data logger. Underwater measurements of light were conducted in the upper 50 m of the water column. The euphotic zone was defined as the layer restricted by a depth of 1% of the surface PAR. The daily PAR was obtained from integration in the LI-1400 module for 5-min intervals (mol quanta m^{-2}) over the all days of study.

2.4. Measurement of fluorescence parameters

Active Chl *a* fluorescence was measured with a MEGA-25 fluorometer (MSU, Russia). The MEGA-25 fluorometer is equipped with high-sensitivity system for registration of chlorophyll fluorescence, and a strong LED source of light for excitation. Three LXHL-PR02 Royal Blue 455-nm LEDs (Luxeon) with light power 700 W each were used. The sample is irradiated by light of equal instantaneous intensity (3000 μmol photons $m^{-2} s^{-1}$) under different pulse widths and intervals, using multiple turnover flashlets. Excitation of the sample with a series of short pulses (5 μs) at long intervals (100 ms) provides a low mean intensity of measuring light, which induces a low level of fluorescence from chlorophyll without inducing photosynthesis. In dark-adapted cells, this first measurement is termed F_0. The sample is then exposed to a long saturating pulse (3000 μmol photons $m^{-2} s^{-1}$ for 1.5 s), and the chlorophyll fluorescence rapidly increases to a maximum (F_m) in dark-adapted cells by triggering the reduction of the PSII primary electron acceptor pool (plastoquinones, Q_a). A photomultiplier (R7400U-20, Hamamatsu) allows recording of the fluorescence with a high time resolution (0.75 μs). Chlorophyll fluorescence was detected at wavelengths above 710 nm (Pogosyan et al., 2009).

Prior to measurement, the samples were kept in the dark for at least 20 min (Schreiber et al., 1994) at ambient temperature. The minimum (F_0) and maximum (F_m) fluorescence of the samples was measured. The maximum dark-acclimated quantum efficiency of PSII (F_v/F_m) was calculated as (Krause and Weis, 1991):

$$F_v/F_m = (F_m - F_0)/F_m \quad (1)$$

Maximum observed F_v/F_m values for phytoplankton under optimum growth conditions are between ca. 0.65 and 0.70 and vary considerably between taxa (Juneau and Harrison, 2005; Suggett et al., 2009b). The F_v/F_m ratio is related to the potential (maximum) photochemical efficiency of PSII and indicates the fraction of the absorbed energy channelled to photosynthesis by PSII reaction centres.

Water samples were exposed in the PAM fluorometer to eight light intensities as for ^{14}C uptake measurements, for 300 s at each step, and steady fluorescence (F_t) and maximum fluorescence (F_m') were measured. The light-acclimated photochemical efficiency of PSII (the effective quantum yield of photochemistry in open reaction centre of PSII, $\Delta F/F_m'$) at a specific actinic irradiance level was calculated as described by Genty et al. (1989):

$$\Delta F/F_m' = (F_m' - F_t)/F_m' \quad (2)$$

where F_m' is the maximum PSII fluorescence in light-acclimated cells, and F_t is the fluorescence yield in actinic light.

Multiplying the number of quanta absorbed by phytoplankton by the value $\Delta F/Fm'$ provides an estimate of the rETR at a specific actinic irradiance level:

$$rETR = \Delta F/F_m' \times E \times 0.5 \quad (3)$$

where E is the actinic light level (μmol photons m^{-2} c^{-1}), and the factor 0.5 is to correct for the partitioning of photons between PSI and PSII, assuming that excitation energy is distributed evenly between the two photosystems (Lippemeier et al., 1999; Schreiber, 2004).

The Chl *a* concentration in the samples where active fluorescence was measured varied from 0.2 to 2.3 mg m^{-3}. The absence of self-shading was checked by diluting a sample 1:1, or some other convenient ratio, and estimating 'fluorescence–concentration' linearity.

2.5. Measurement of abundance and biomass of phytoplankton

Luminescent microscopy was used to count small phytoplankton forms (linear size < 10–15 μm). Water samples (25–50 ml) were stained with fluorochrome primulin (Direct Yellow 59, Sigma-Aldrich Co.), fixed with 3.6% glutaraldehyde solution and filtered through black 0.4-μm pore-size Nuclepore filters (Grebecki, 1962; Hobbie et al., 1977; Caron, 1983), applying our own modification of the method (Sazhin et al., 2007). Just after preparation, samples were frozen and stored at −24 °C until analysis. Samples were analysed with a Leica DM 500B microscope at magnifications of 200–1000. Small numerous forms were counted in 50–100 fields of vision, and rare organisms were observed at total viewing of samples.

For the enumeration of large phytoplankton forms, water samples were concentrated by the inverse filtration method. Water samples (50–70 ml) were filtered through a 1 μm Nuclepore filter and then fixed with 0.5–1% formalin (Sukhanova, 1983). Identification of species and counting of cells were carried out with a Leica DM2 500 light microscope at magnifications of 100–400. Naujotte (0.1 ml) and Naumann (1.0 ml) counting chambers were used. During the microscopy investigations, cells were taken into account at the stage of spore formation. This allowed us to determine separately the abundance and biomass of spores and non-spores of diatom algae. Diatom non-spores are further named 'active diatoms'. The constructive metabolism type of different algae species was determined by reference to the literature (Tomas, 1997; Throndsen et al., 2007).

The wet biomass was calculated by the method of geometric similarity, equating cells to corresponding shapes (cylinder, sphere, ellipsoid of rotation) (Sun and Liu, 2003). Conversion of phytoplankton biomass into carbon was carried out by following allometric relationships (Menden-Deuer and Lessard, 2000).

2.6. Statistical analysis

Standard statistical methods of descriptive, correlation and *t*-test analyses were used. Averages in the text below are presented with a standard deviation (± SD). Correlation is given with the coefficient of correlation (r), number of measurements (n) and the probability of the null hypothesis (p).

3. Results

3.1. Research area hydrological peculiarities

From the results of analysis of TS plots based on CTD data, five areas with different hydrological conditions were defined. Groups of stations with similar parameters of the water column were chosen along parallel sections through the central and eastern branches of the St Anna Trough. A brief description of these areas is given below.

(1) The Shallow Yenisei shelf (stations 5010, 5020, 5023, 5024 and 5025; depths 30–50 m) was under the influence of river discharge. Freshening of surface waters reached 18.0.
(2) Slight desalination of the surface was observed over the eastern shallow shelf (stations 5028, 5029, 5030 and 5032; depths 40–60 m); the salinity of upper mixed layer was not less than 24.0.
(3) The central continental shelf adjacent to the St Anna Trough

(stations 5026, 5033 and 5043; depths 70–140 m) was apparently influenced by waters of Atlantic origin. In this area, temperature at a depth of 35–55 m increased by 0.2–0.6°C. At station 5033 at the same depths, temperature was positive when salinity increased until 34–34.2.

(4) An abrupt frontal zone between the shallow shelf and deep sea was observed over the edge of the continental shelf with drastic changes of the depths (stations 5034, 5035, 5044, 5047, 5048 and 5049; depths 160–320 m). The salinity gradient of the surface 20-m layer was 5.5 at a distance of 30 km, and active interaction among Atlantic origin water, Barents Sea water and Kara Sea water was fixed. The same situation had been described previously (Rudels et al., 2004).

(5) The St Anna Trough slope with a smooth change of depth (stations 5037, 5039, 5041, 5042, 5045 and 5046; depths 350–540 m) was influenced by Atlantic water. At depths of 30–35 m, there was a layer with temperature between +0.5 and + 1°C and high salinity (34.0–34.5). This layer in comparison with the surface was enriched by nitrate (up to 13 μM) and phosphate (up to 1 μM). In the eastern branch of the St Anna Trough slope, the vertical stratification was much more drastic, and the salinity gradient was 0.4–0.5, while it did not reach 0.1 in the central branch.

Sampling positions in the study areas are demonstrated on the map (Fig. 1).

3.2. Incident irradiance in the research area

The studies were realized in the one and a half months before polar night, during a noticeable decrease in day length (from 13.7 to 11.3 h). The maximum number of cloudy days (80%) and the minimum number of clear days (10%) is noted at the 76° N latitude in autumn before polar night (on November 3) (Gavrilova, 1963). It reduces such small flux of solar radiation at this time. For an annual cycle of total solar radiation, a very small part of it is in September in the Kara Sea (Fig. 2). During our study, solar radiation at the sea surface varied from 1.93 to 11.28 mol photons m^{-2} day^{-1} (average: 4.03 ± 2.81 mol photons m^{-2} day^{-1}; sum for 20 days: 91.89 mol photons m^{-2} day^{-1}). Accepting total solar radiation in a year in the Kara Sea as 12,300 mol photons m^{-2} day^{-1} (Gavrilova, 1963), total solar radiation during our study was about 0.7% of annual. Thus, under the terms of irradiance, we can consider this period as the end of the growth season. Incident PAR decreased rapidly further north due to decreasing day length and solar elevation angle.

The depth of the euphotic zone, i.e. the depth of penetration of 1% of surface irradiance, varied from 5 to 30 m within the study area.

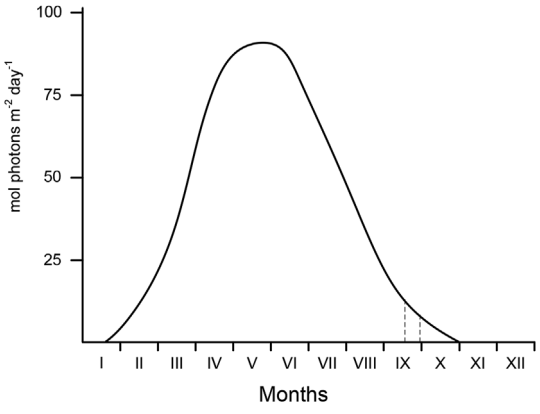

Fig. 2. Total (direct and scattered) solar radiation at 76° N (Gavrilova, 1963). The dotted line designates the beginning and end of our studies.

3.3. Photophysiology and productive parameters

The quantum yield of PSII in surface samples was high at all stations (0.55–0.71) except coastal station 5010, where a low surface F_v/F_m value (0.32) was detected. This low value was likely due to inhibition of brackish phytoplankton by higher surface salinity (26.3) as compared with other coastal stations (17.7–24.6). The highest surface F_v/F_m (0.71) was detected at the coastal station 5020 near the Yenisei estuary and at the shelf-edge station 5037. Most profile stations showed a constant or slight decrease in F_v/F_m, with a depth within the 0–25-m layer, and the main decrease was below 30 m. In contrast, in some stations there was a gradual decrease in F_v/F_m with depth. The last stations were in a zone with a strong vertical gradient of salinity and temperature caused by the eastern Novaya Zemlya Current and Yamal Current (St. 5033, 5034, 5037 and 5043) and the current along the Taimyr (St. 5023, 5028, 5029 and 5030). Thus, at all stations, the maximal F_v/F_m value was detected on the surface or within the upper 25 m. This is also represented in the similar F_v/F_m vertical profiles among the sub-regions, irrespective of differences in phytoplankton biomass and composition.

Chl *a* concentrations ranged between 0.02 and 1.49 mg m^{-3}, with higher values in the surface or subsurface layers than in the deeper layers. The highest surface Chl *a* concentrations (1.35–2.39 mg m^{-3}) were determined over the shelf edge in the central branches in the St Anna Trough (St. 5043, 5044 and 5049). The lowest surface Chl *a* concentrations (0.20–0.45 mg m^{-3}) were detected in the central area of the coastal zone (St. 5010, 5024, 5029 and 5032). In half the stations, the vertical Chl *a* distribution was characterized by a subsurface chlorophyll maximum under the UML (10–20 m depth), with a gradual decrease in Chl *a* concentrations below the UML. In other stations, there was a gradual decrease in Chl *a* concentrations within the UML to minimal values (< 0.07 mg m^{-3}).

The rETR in PSII within the euphotic zone varied from 0.10 to 38.00 a.u. At all stations, rETR decreased exponentially with depth, related to the decrease in underwater light. The surface rETR values were more changeable and varied in a wide range from 4.87 to 38.0. The highest surface rETR values (28.3–38.0) were found in the continental central shelf (depths 48–60 m) at stations 5025, 5026 and 5032. The lowest surface rETR values (4.87–9.67) were found at the deepest stations in both branches in the St Anna Trough (St. 5041, 5042, 5045 and 5046, depths more than 400 m).

The vertical distribution of all values of the main primary productive parameters is shown in Fig. 3. It is obvious that most F_v/F_m values within the upper 20 m were in the range 0.5–0.7 (Fig. 3a). In the 20–30-m layer, the F_v/F_m range was widened towards low values. In the deeper layer, there was a downtrend. This distribution shows that the maximal quantum yield of photochemistry in the phytoplankton had high potential from the surface to 30 m depth. The depth-specific maximal Chl *a* concentrations decreased exponentially with depth (Fig. 3b). The highest values were in the upper 18 m. In deeper layers, the Chl *a* concentration did not exceed 0.5 mg m^{-3}. The highest rETR values (more than 10.0) were in upper 0–3-m layer of the water column (Fig. 3c). At depths of 3–10 m, more than 80% of rETR values were in the range of 0–5.0.

Fig. 4 shows data for the effective photochemical efficiency of PSII in actinic light ($\Delta F/F_m'$) compared with rETR calculated from it for surface samples. $\Delta F/Fm'$ varied from 0.095 to 0.436, reflecting the different efficiency with which absorbed light drives photochemistry at various stations. Variability of $\Delta F/F_m'$ and rETR differed because of changeable light intensity. In particular, at stations 5024, 5025 and 5026 (northern part of the coastal shelf), we detected medium $\Delta F/F_m'$ values and high rETR values caused by higher light intensity (125–220 μmol photons m^{-2} s^{-1}) relative to other sites (20–87 μmol photons m^{-2} s^{-1}). From these two parameters, rETR was used in this study as a qualitative characteristic of activity of the initial ('light') photosynthesis stage that is the energy flow for biosynthesis.

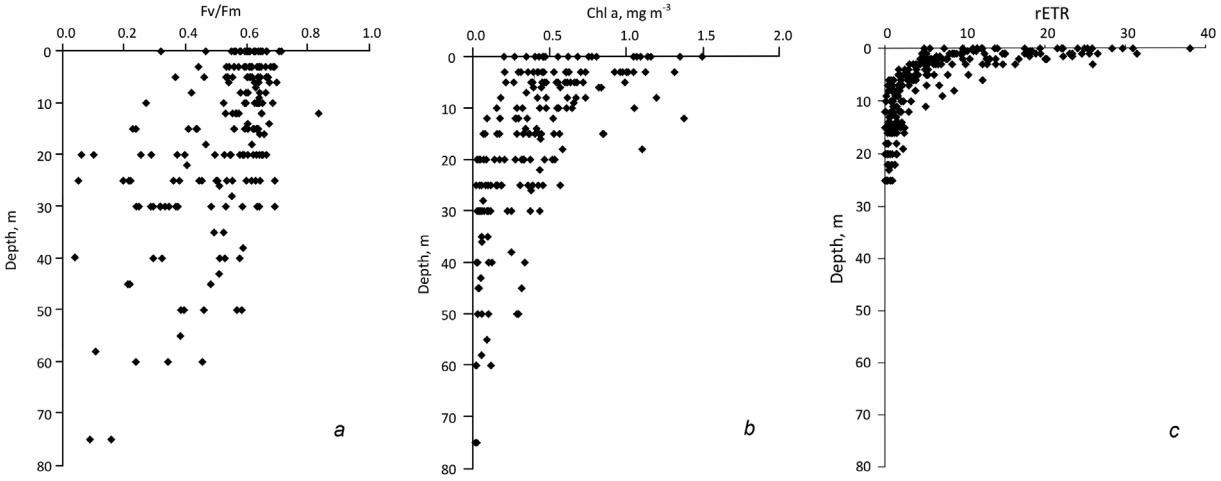

Fig. 3. Vertical distribution of phytoplankton state parameters: a) maximum quantum efficiency of PSII, F_v/F_m, b) chlorophyll *a,* c) relative electron transport rate, rETR.

Analysis of the relationship between rETR and P^B in the euphotic zone under the same irradiance levels shows a strong positive correlation (r = 0.78, n = 310, P = 0.05) (Fig. 5).

The maximum photosynthetic activity of phytoplankton, expressed in terms of rETR, during our study was in the surface layer (0–3 m) of the water column (Fig. 3c). In the same layer, there was also the widest range of rETR and P^B values, which is important for assessment of their variability and the relation between these parameters. At other depths (deeper than 3 m), P^B values were low (less than 0.25 mg C (mg Chl $a)^{-1}\,h^{-1}$), which could lead to a high degree of error in estimating variability in the comparative analysis of rETR and P^B values. Therefore, the following analysis of photosynthetic efficiency was carried out for surface data, which characterize the structure and functional activity of phytoplankton in the five allocated areas.

Average values for biological parameters in surface waters are presented in Table 1.

P^B in surface waters (P_0^B) varied from 0.14 to 1.91 (average 0.67 ± 0.47 mg C (mg Chl $a)^{-1}\,h^{-1}$). Similar to the surface rETR ($rETR_0$) distribution, the highest P_0^B values (> 1.0 mg C (mg Chl $a)^{-1}\,h^{-1}$) were found at stations 5025, 5026 and 5032, with total depths of 30–60 m (coastal shelf) (Fig. 6b). The lowest P_0^B values (< 0.2 mg C (mg Chl $a)^{-1}\,h^{-1}$) were found over the shelf edge at stations 5044–5049 in the central branch in the St Anna Trough (depths more than 160 m) and at stations 5041–5042 in a deep-water part of the eastern branch.

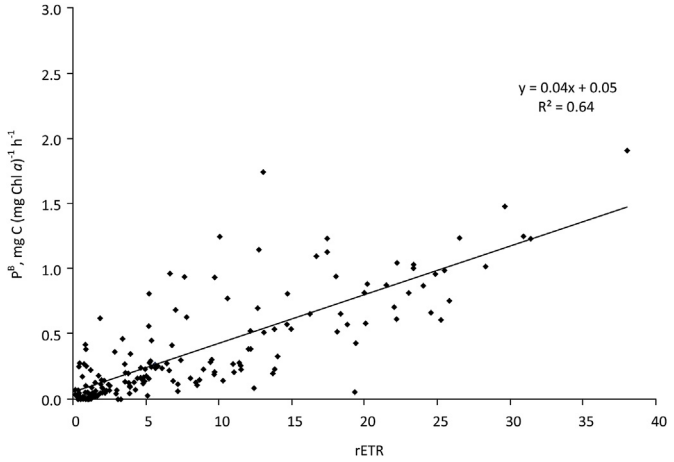

Fig. 5. Relationship between primary production, P^B, and relative electron transport rate, rETR, in the euphotic zone throughout the entire study area.

Irradiance, salinity, temperature and nutrients (mineral nitrogen, phosphates and silicates) as well the contribution of the five different groups of microalgae (autotrophic dinoflagellates, active diatoms, autotrophic flagellates, diatom spores and heterotrophs) to the total phytoplankton biomass have been considered as the most significant

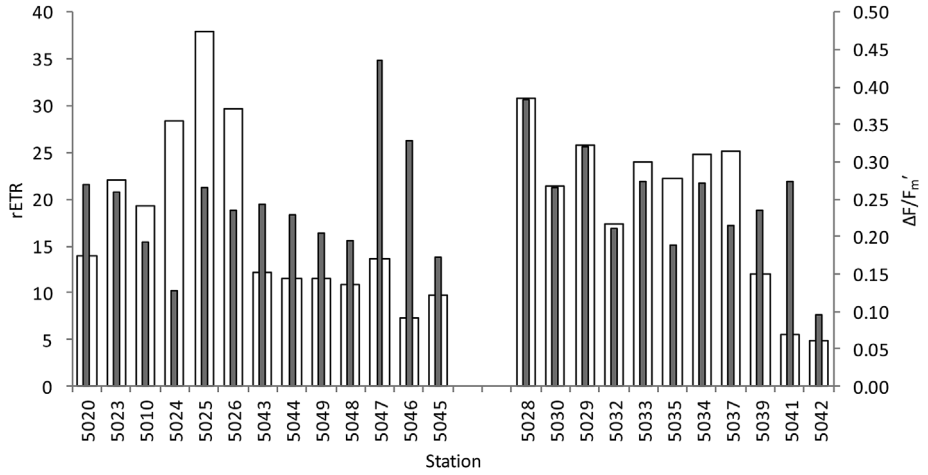

Fig. 4. Effective quantum yield of PSII ($\Delta F/F_m'$, grey) and relative electron transport rate (rETR, white) for surface samples.

Table 1
Biological parameters (average and standard deviation) for different regions in surface waters (0 m).

Area	Date	Depth	$rETR_0$	P_0^B	F_v/F_m	Chl *a*	% Phaeo	%DINO	%DIA	%DIA spore	%FLA	%HET
Yenisei shelf	17–22 Sept	36 ± 8	24.3 ± 9.2	0.80 ± 0.72	0.59 ± 0.15	0.80 ± 0.37	23 ± 4	5 ± 5	48 ± 20	2 ± 2	18 ± 9	26 ± 15
Eastern shelf	23–24 Sept	48 ± 10	23.9 ± 5.8	1.03 ± 0.25	0.58 ± 0.08	0.41 ± 0.25	34 ± 6	38 ± 31	33 ± 34	10 ± 12	7 ± 2	12 ± 7
St Anna shelf	22, 25, 28 Sept	110 ± 40	21.9 ± 8.9	0.96 ± 0.48	0.61 ± 0.02	0.99 ± 0.44	27 ± 6	20 ± 16	13 ± 18	0	27 ± 16	40 ± 16
Edge of St Anna shelf	25, 28–29 Sept	220 ± 57	15.8 ± 6.1	0.42 ± 0.30	0.61 ± 0.03	1.22 ± 0.59	31 ± 2	35 ± 18	11 ± 10	2 ± 5	26 ± 14	25 ± 15
St Anna slope	25–26, 29 Sept	433 ± 82	10.8 ± 7.5	0.32 ± 0.17	0.62 ± 0.06	0.49 ± 0.05	28 ± 3	22 ± 12	6 ± 9	2 ± 3	35 ± 15	34 ± 6

Notes: depth – total depth (m); $rETR_0$ – relative electron transport rate; P^B – biomass-specific primary production (mg C (mg Chl *a*)$^{-1}$ h^{-1}); F_v/F_m – PSII efficiency; Chl *a* – concentration of chlorophyll *a* (mg m^{-3}); % Phaeo – contribution of phaeophytin a in the total concentration of Chl *a* + Phaeo; share of different algae groups in the total phytoplankton biomass (%): %DINO – autotrophic dinoflagellates, %DIA – active diatoms, %DIAspore – diatom spores, %FLA – flagellates, %HET – heterotrophs.

factors impacting values and distribution of $rETR_0$ (see Figs. 1 and 2 in Mosharov et al., submitted).

The correlation analysis of all considered parameters in surface waters throughout the entire study area revealed relationships between $rETR_0$ and daily incident PAR, salinity and diatom share in the total biomass of phytoplankton (Table 2).

A strong positive correlation (r = 0.8, n = 23, P = 0.05) was observed between rETR and average-day incident PAR (Fig. 7a). When calculating rETR, an appropriate PAR value was used. Therefore, it is evident that higher rETR values occurred if there was a higher light level. However, at similar light intensities, the rETR values differed greatly, likely characterizing the photophysiological features of phytoplankton at each station (Fig. 7a). F_v/F_m was unaffected by PAR (Fig. 7b).

A strong positive correlation was found between the share of active diatoms and $rETR_0$ values (r = 0.58, n = 23, P = 0.05). An increase in the share of diatoms in the total phytoplankton biomass caused an increase in rETR. A high mean share of diatoms in the shelf areas was followed by high mean $rETR_0$ values (Table 1). On the shelf edge and slope, both the mean values of the share of diatoms in phytoplankton biomass and mean $rETR_0$ values were low.

It should be noted that there was a negative correlation between $rETR_0$ or P_0^B and the share of autotrophic flagellates in total phytoplankton biomass. The decrease in the level of productive activity with an increase in the relative abundance flagellates can be explained by a decrease in the share of diatoms in the community. Distribution of these microalgae groups had a strong negative correlation (r = −0.74, n = 23, P = 0.05). An increase in the share of flagellates followed a reduction of the diatom share in the phytoplankton community and vice versa (Tables 1 and 2).

A negative correlation was observed between salinity and $rETR_0$ (r = −0.51, n = 23, P = 0.05) – a higher $rETR_0$ corresponded to areas with fresher waters.

Perhaps the influence of salinity on rETR is caused by a decrease in the diatom share in the total biomass of phytoplankton with an increase of salinity (Tables 1 and 2), and diatoms determine the total level of productive activity in this area. Salinity influences diatom growth indirectly. A freshening level (decrease in salinity) in surface waters reflects the influence of river waters, characterized by an increase in the content of nutrients, especially silicates, providing diatom growth. The silicate concentration was negatively correlated with salinity (Tables 1 and 2).

In the surface layer, the total content of mineral nitrogen (DIN = NO_2 + NO_3 + NH_4) varied in the range 0.42–2.13 μM; for phosphates, the range was 0.04–0.44 μM, and for silicon it was 0.12–30.65 μM. Correlations among nutrient and rETR values were not obvious at the surface throughout the entire study area (Table 2). Within the local areas, however, a positive trend between $rETR_0$ and DIN (for the Yenisei shelf and eastern shallow shelf) and between $rETR_0$ and DIN/PO_4 (for the edge and slope areas in the St Anna Trough) has been revealed (Fig. 8). For other nutrients, the same trends have not been revealed. It should be noted that these relationships are statistically unreliable due to the lack of measurements there.

4. Discussion

The values of P_0^B observed compare with those previously reported for Arctic (0.83–1.12 mg C (mg Chl *a*)$^{-1}$ h^{-1} in the Chukchi Sea in summer (Hill and Gota, 2005); 0.72–2.45 mg C (mg Chl *a*)$^{-1}$ h^{-1} in the Gulf of Alaska (Peterson, 2011)) and Antarctic seas (0.19–2.41 mg C (mg Chl *a*)$^{-1}$ h^{-1} in the shallow bay of Potter Cove (Schloss, 2002); 0.13–2.23 mg C (mg Chl *a*)$^{-1}$ h^{-1} in the Indian Ocean sector (Jacques, 1983)). Relatively low values have been reported for the polar front of the Indian Ocean sector of the South Ocean during the austral summer:

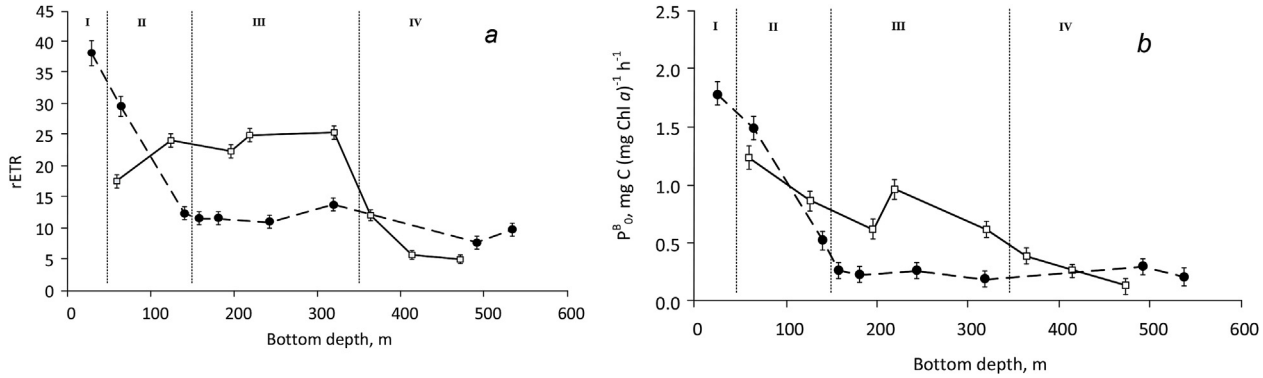

Fig. 6. Variation in surface rETR (a) and primary production, P_0^B (b) in areas with different hydrological conditions along sections in the central (circles) and eastern (squares) branches in the St Anna Trough: *I* – coastal, *II* – shelf, *III* – shelf edge, *IV* – slope.

Table 2
Correlation matrix between abiotic and biological parameters in surface waters.

Spearman rank order correlations MD pairwise deleted. Marked correlations are significant at P < 0.05000.

	$rETR_0$	P_0^B	PAR_{av}	Sal UML	T UML	% Dino	% Dia	% Flag	DIN	PO_4	DIN/PO_4	SiO_3
$rETR_0$	1.00	**0.80**	**0.80**	**−0.51**	**0.42**	0.02	**0.58**	**−0.52**	0.33	0.39	−0.39	**0.50**
P_0^B	**0.80**	1.00	**0.75**	**−0.42**	0.30	0.08	0.37	**−0.49**	0.20	0.35	−0.36	**0.42**
PAR_{av}	**0.80**	**0.75**	1.00	−0.17	0.21	0.16	**0.46**	**−0.58**	−0.07	0.18	−0.35	0.22
Sal UML	**−0.51**	**−0.42**	−0.17	1.00	**−0.67**	0.27	**−0.47**	0.39	**−0.44**	**−0.85**	**0.70**	**−0.91**
T UML	**0.42**	0.30	0.21	**−0.67**	1.00	−0.41	0.28	−0.17	−0.04	**0.49**	**−0.60**	**0.72**
% Dino	0.02	0.08	0.16	0.27	−0.41	1.00	−0.22	−0.14	0.05	−0.16	0.13	−0.38
% Dia	**0.58**	0.37	**0.46**	**−0.47**	0.28	−0.22	1.00	**−0.74**	0.08	0.40	**−0.45**	0.35
% Flag	**−0.52**	**−0.49**	**−0.58**	0.39	−0.17	−0.14	**−0.74**	1.00	0.06	−0.39	**0.55**	−0.31
DIN	0.33	0.20	−0.07	**−0.44**	−0.04	0.05	0.08	0.06	1.00	0.39	0.09	0.41
PO_4	0.39	0.35	0.18	**−0.85**	**0.49**	−0.16	0.40	−0.39	0.39	1.00	**−0.84**	**0.80**
DIN/PO_4	−0.39	−0.36	−0.35	**0.70**	**−0.60**	0.13	**−0.45**	**0.55**	0.09	**−0.84**	1.00	**−0.68**
SiO_3	**0.50**	**0.42**	0.22	**−0.91**	**0.72**	−0.38	0.35	−0.31	0.41	**0.80**	**−0.68**	1.00

Notes: $rETR_0$ – relative electron transport rate; P_0^B – biomass-specific primary production (mg C (mg Chl *a*)$^{-1}$ h^{-1}); PAR_{av} – average-day incident light (μmol photons m^{-2} day^{-1}); Sal UML – salinity in the upper mixed layer; T UML – water temperature in the upper mixed layer (°C); share of phytoplankton groups in the total carbon biomass (%): %Dino – dinoflagellates, %Dia – diatoms, %Flag – flagellates; nutrient data: DIN – dissolved inorganic nitrogen (DIN = NO_2 + NO_3 + NH_4, μM), PO_4 – dissolved inorganic phosphorus (μM), DIN/PO_4 – molar nitrogen–phosphorus ratio, SiO_3 – dissolved inorganic silicon (μM).

0.67–0.84 mg C (mg Chl *a*)$^{-1}$ h^{-1} (Tripathy, 2015). As shown in previous studies (Mosharov, 2010; Demidov et al., 2014, 2017; Mosharov et al., 2016), P_0^B values in the Kara Sea (August–September) vary from 0.8 to 2.32 mg C (mg Chl *a*)$^{-1}$ h^{-1} in the southwestern region, from 0.46 to 2.59 mg C (mg Chl *a*)$^{-1}$ h^{-1} in the Yenisei estuary and river runoff zone, and from 0.38 to 1.49 mg C (mg Chl *a*)$^{-1}$ h^{-1} in the northern region.

The rETRs resembled those for phytoplankton in the Chukchi Sea off Point Barrow, Alaska (from 4 to 50; Manes, 2009) and in the North Sea and South Atlantic (2–40; Röttgers, 2007). Similar data (10–50) were reported by Schreiber (1998) for phytoplankton from Sydney Harbour.

The study was carried out in the period of low solar radiation caused by a noticeable decrease in day length and solar elevation angle. Hence, not enough light penetrates into the depth of the water column, so the main productive activity of phytoplankton is linked to the surface layer. Total solar radiation during our study was about 0.7% of annual; therefore, this period can be considered as the end of the growth season for phytoplankton under light conditions.

Low values for Kara Sea primary production at the end of the growth season are caused by a general reduction of incident solar radiation in September–October at high latitudes. Apparently, low PAR limits primary production more than low nutrients in the photosynthetic layer and defined low (< 100 mg C m^{-2} day^{-1}) integral PP in many Kara Sea areas (Demidov et al., 2014). The maximal rate of primary production at most stations in the Kara Sea (27 stations out of 38 in total) in September 2011 was observed in the surface layer; for the rest of them, it was within the upper 0–3 m (Mosharov et al., 2016). The spatial variability of P_0^B in the studied areas is close to the pattern based on averaged long-term values for the Kara Sea (0.46–2.32 mg C (mg Chl *a*)$^{-1}$ h^{-1} (Demidov et al., 2014).

Despite the low P^B, the potential for phytoplankton photosynthetic activity determined by the maximum quantum efficiency of PSII (F_v/F_m) was high in the upper 30-m layer of the water column. Similar vertical profiles and relatively high F_v/F_m are found among different sub-regions across the western Antarctic Peninsula in late summer (Russo et al., 2018). This indicates a high degree of physiological plasticity, even considering different phytoplankton communities and the large spatial variability of physical water column features.

The bulk of Chl *a* was concentrated in the upper 18-m layer of the water column, with the maximum values at the surface (see Fig. 3). However, realization of productive potential was observed only in the surface layer of the water column. The rETR values, representing the rate of solar energy transition into the chemical energy of a cell, providing processes of biosynthesis of organic matter by phytoplankton, were at a maximum in the surface layer. P^B in the surface layer were more changeable (a difference between minimum and maximum P^B values of 14 times) than rETR (8 times) which can reflect, apparently, a greater influence of changing environmental factors on the efficiency of using of absorbed light energy in biosynthesis processes.

To determine the rETR values for each sample, we set the light level which corresponded with the native one. During our study, the light level varied with weather conditions (cloudy or clear sky) and in

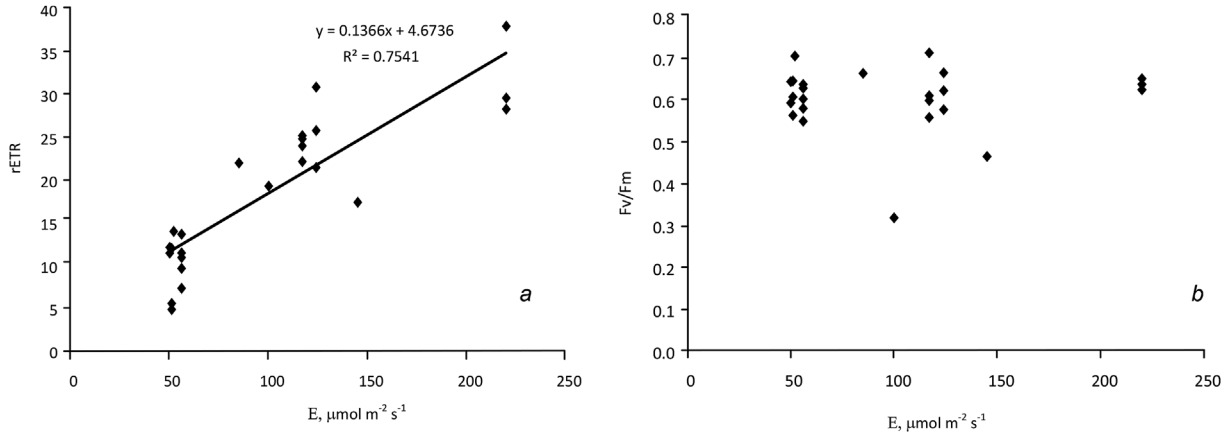

Fig. 7. Variability of relative electron transport rate, rETR (a) and PSII efficiency, F_v/F_m (b) depending on actual average-day incident PAR.

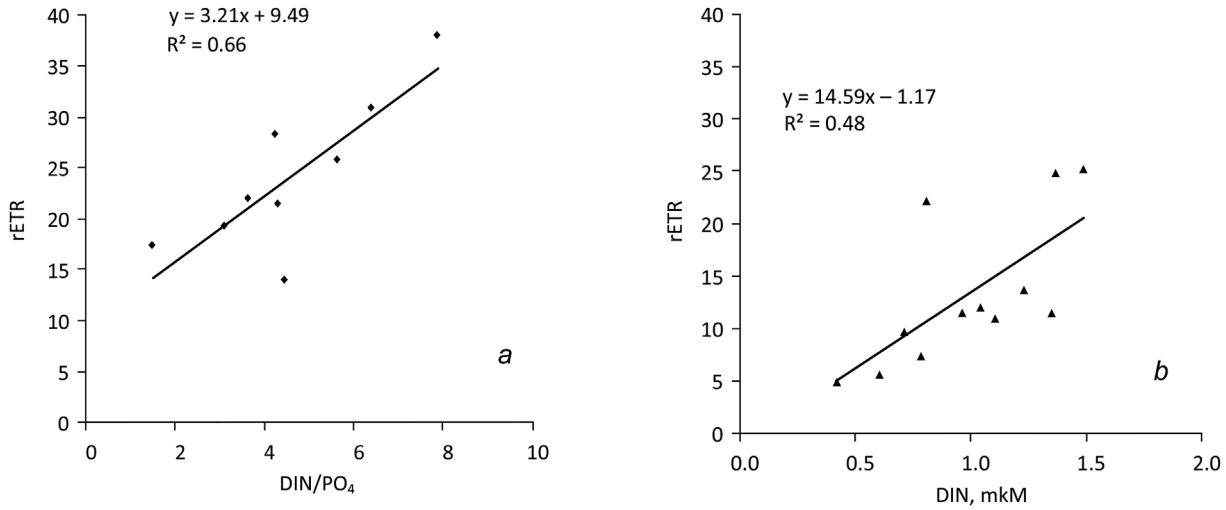

Fig. 8. Relationship between relative electron transport rate values, $rETR_0$, and DIN/PO_4 over the Yenisei shelf and the eastern shallow shelf (a), and DIN over the edge and slope in the St Anna Trough (b).

connection with decreasing solar elevation angle with every following day. By definition, the rETR value is proportionally to light intensity. Hence, comparison of rETR values at different sites (under different light intensities) does not permit the identification of physiological features of variability of this parameter which characterize the activity of the light stage of photosynthesis. The ratio of rETR and P^B measured under similar light intensities for each sample allows us to compare the photosynthetic performance of phytoplankton at different sites irrespective of the current light conditions.

Between the productive parameters considered in this study – rETR and P^B – a close relationship was observed ($r = 0.8$, $P = 0.05$) in the surface layer ($n = 23$) and for the whole data set ($n = 310$). That allows consideration of them as values reflecting the intensity of different stages of photosynthesis – light and dark stages, respectively. Linear correlations have been documented between ETR and gross C fixation and/or O_2 production across different regions (Kromkamp et al., 2008; Suggett et al., 2009a; Lawrenz et al., 2013).

The photosynthetic efficiency ($P^B_0/rETR_0$) calculated for each station at the surface (0 m) varied from 0.014 to 0.071 (average 0.034 ± 0.012). Our results were in the approximately same range as those found for estuarine phytoplankton and microphytobenthos (Barranguet and Kromkamp, 2000), where values the rETR efficiency for C fixation (EE) varied between 0.04 and 0.16. These authors recalculated published data for cultures and gave EE values varying between 0.007 and 0.02 for different marine phytoplankton species.

The maximum value of this parameter was at station 5032 near the eastern shelf whereas for other areas this value did not exceed 0.05

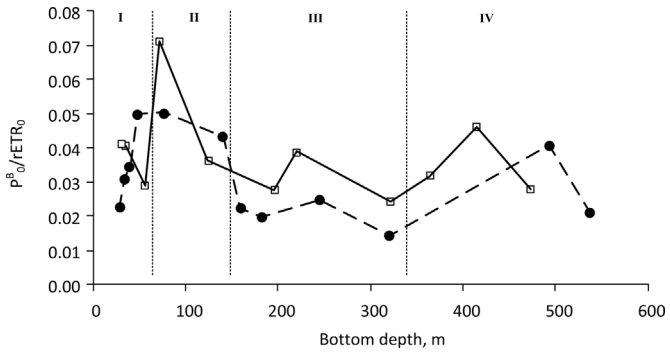

Fig. 9. Variability of $P^B_0/rETR_0$ in areas with different hydrological conditions along sections in the central branch (circles) and eastern branch (squares) in the St Anna Trough: *I* – coastal, *II* – shelf, *III* – shelf edge, *IV* – slope.

(Fig. 9). As shown in Fig. 9, spatial distribution of $P^B_0/rETR_0$ parameters along the sections in the central and eastern branches out of the shelf zone (depths more than 150 m) was similar. In the direction from the coast to a deep-water area in the St Anna Trough, the areas with high values for this parameter were allocated over the external coastal area (St. 5025 and 5032), over the central shelf (St. 5026 and 5043) and over the continental slope in both branches (St. 5041 and 5046) of the St Anna Trough. At the same time, in the central branch of the St Anna Trough, photosynthetic efficiency decreased in comparison with the eastern branch though time studies in both branches differed only for 3 days (in the first case for 28–29 September, in the second for 25–26 September). It is obvious that at the end of growth season when the level of solar radiation approaches a seasonal minimum (Fig. 3), a daily decrease in the light level is significant for photosynthetic efficiency.

Empirical evidence from a range of aquatic systems demonstrates a linear relationship between ETR and rates of C fixation and/or O_2 production; however, deviation from linearity has also been reported (Suggett et al., 2009a; Hancke et al., 2015). Deviations are reported under extreme conditions such as very high or low light conditions, extreme temperature, or nutrient stress (Flameling and Kromkamp, 1998; Hancke et al., 2008; Napoleon et al., 2013). In some studies, the interrelations between ETR and C fixation/O_2 production have also been shown to be species-specific (Suggett et al., 2009a).

Despite a decrease in illumination level, and following a reduction in productive characteristics of the phytoplankton community at the end of a growth season, the role of diatoms in efficiency remains a major one in the eastern Kara Sea. A strong positive correlation between the share of active diatoms and rETR values was noted. The share of diatoms in the plankton community at the surface was more closely related to the level of water freshening and the maintenance of nutrients than for other groups of algae. In local areas, positive trends between rETR values and DIN concentrations (over the Yenisei and eastern shallow shelves) and between rETR values and DIN/PO_4 relations (over the edge and slope areas in the St Anna Trough) have been revealed. Most likely, the reaction of diatoms to changing abiotic factors defines the variability of productive characteristics of the phytoplankton community in the eastern Kara Sea in autumn. It should be noted that the spring increase in productive characteristics of phytoplankton in the Kara Sea is firstly connected with diatom bloom (Makarevich et al., 2015). The same studies were not carried out during late autumn.

Areas with an increased $P^B_0/rETR_0$ ratio are characterized by drastic gradients of hydrophysical conditions caused by different factors in each case. The external shelf area (St. 5025, 5026, 5032 and 5043) is a

region where saline water is freshened by the spread of Yenisei River runoff (Zatsepin et al., 2010a). At the same time, increased water temperature was observed in the surface layer in this area. A strong frontal zone is formed over the shelf edge (St. 5034 and 5048) where two currents (the eastern Novaya Zemlya Current and Yamal Current) merge and spread along the 100-m isobath to the northeast (Zatsepin et al., 2010a). In a deep-water zone over the continental slope in both the western and central branches in the St Anna Trough (St. 5041 and 5046), an upwelling – raising of the Atlantic waters to the top layers – is formed. The increase of phytoplankton productive activity in frontal zones of the Yamal Current was defined by us as well in previous works in the Kara Sea in 2007 (Mosharov, 2010).

In spite of the fact that the depth of the euphotic zone varied from 5 to 30 m, and high Chl *a* concentrations were in the upper 18-m layer, the maximum photosynthetic activity of planktonic microalgae has been defined in the narrow upper 3-m layer. It is obvious that in the deeper layers (lower than 3 m), Chl *a* was inactive. At the same time, as shown in our previous works (Sukhanova et al., 2015a; Sergeeva et al., 2016), the community of planktonic microalgae in subsurface layers (deeper than 3 m), was at a stage of sporification that is typical of the final stage of seasonal succession of phytoplankton.

5. Conclusions

A close connection between the parameters of primary production – rETR and P_0^B – reflecting the intensity of the light and dark stages of photosynthesis has been revealed.

In the eastern Kara Sea at the end of a growth season, rETR depends on the daily incident PAR and the share of diatoms in the total phytoplankton biomass. Despite a decrease in light level and following a reduction in the values of productive characteristics of the phytoplankton community, diatoms continue to play a major role in primary productivity in the eastern Kara Sea during this period.

Photosynthetic performance, reflecting the extent of the use of absorbed light energy in processes of the synthesis of organic matter, expressed as $P_0^B/rETR_0$ ratio, increased in areas with drastic gradients of hydrophysical conditions over the external shelf, the shelf edge and in a deep-water area over the continental slope in the St Anna Trough.

Acknowledgments

We thank the deputy director of Shirshov Institute of Oceanology, Russian Academy of Sciences, M. Flint, for organization and research leadership of the expedition in the Kara Sea, and A. Demidov for providing primary production measurement and comments to the manuscript.

Funding: this work was performed in the framework of the state assignment of Ministry of Science and Higher Education of the Russian Federation (theme No. № 0149-2019-0008, processing and analysis of productivity data, preparation of publication) and supported by the Russian Foundation for Basic Research (grants no. 16-35-60068 young_a_dr, and 18-05-00326, processing and analysis of phytoplankton data; grant no. 18-05-60069, hydrophysical and hydrochemical data processing and analysis).

The authors are grateful to anonymous referee for very valuable critical comments and the editing of the paper.

References

Alderkamp, A.-C., Garcon, V., de Baar, H.J.W., Arrigo, K.R., 2011. Short-term photoacclimation effects on photoinhibition of phytoplankton in the drake passage (southern ocean). Deep Sea Res. Part I 58, 943–955. https://doi.org/10.1016/j.dsr.2011.07.001.

Alderkamp, A.-C., Kulk, G., Buma, A.G.J., Visser, R.J.W., Van Dijken, G.J., Mills, M.M., Arrigo, K.R., 2012. The effect of iron limitation on the photophysiology of *Phaeocystis antarctica* (Prymnesiophyceae) and *Fragilariopsis cylindrus* (Bacillariophyceae) under dynamic light. J. Phycol. 48, 45–59. https://doi.org/10.1111/j.1529-8817.2011.01098.x.

Alexander, V., 1995. The influence of the structure and function of the marine food web on the dynamics of contaminants in Arctic Ocean ecosystems. Sci. Total Environ. 160/161, 593–603.

Badger, M.R., von Caemmerer, S., Ruuska, S., Nakano, H., 2000. Electron flow to oxygen in higher plants and algae: rates and control of direct photoreduction (Mehler reaction) and rubisco oxygenase. Phil. Trans. Roy. Soc. Lond.: Series B 355, 1433–1446. https://doi.org/10.1104/pp.114.238238.

Barranguet, C., Kromkamp, J., 2000. Estimating primary production rates from photosynthetic electron transport in estuarine microphytobenthos. Mar. Ecol. Prog. Ser. 204, 39–52. https://doi.org/10.3354/meps204039.

Beardall, J., Young, E.B., Roberts, S., 2001. Approaches for determining phytoplankton nutrient limitation. Aquat. Sci. 63, 44–69. https://doi.org/10.1007/PL00001344.

Bergmann, T., Richardson, T.L., Paerl, H.W., Pinckney, J.L., Schofield, O., 2002. Synergy of light and nutrients on the photosynthetic efficiency of phytoplankton populations from the Neuse River Estuary, North Carolina. J. Plankton Res. 24, 923–933. https://doi.org/10.1093/plankt/24.9.923.

Brugel, S., Nozais, C., Poulin, M., Tremblay, J.E., Miller, L.A., Simpson, K.G., Gratton, Y., Demers, S., 2009. Phytoplankton biomass and production in the southeastern Beaufort Sea in autumn 2002 and 2003. Mar. Ecol. Prog. Ser. 377, 63–77. https://doi.org/10.3354/meps07808.

Bukhov, N., Carpentier, R., 2004. Alternative Photosystem I-driven electron transport routes: mechanisms and functions. Photosynth. Res. 82, 17–33. https://doi.org/10.1023/B:PRES.0000040442.59311.72.

Carmack, E.C., 2007. The alpha/beta ocean distinction: a perspective on freshwater fluxes, convection, nutrients and productivity in high-latitude seas. Deep Sea Res. Part II 54, 2578–2598. https://doi.org/10.1016/j.dsr2.2007.08.018.

Caron, D.A., 1983. Technique for enumeration of heterotrophic nanoplankton using epifluorescence microscopy, and comparison with other procedures. Appl. Environ. Microbiol. 46, 491–498. http://aem.asm.org/content/46/2/491.full.pdf+html.

Demidov, A.B., Kopelevich, O.V., Mosharov, S.A., Sheberstov, S.V., Vazyulya, S.V., 2017. Modelling kara Sea phytoplankton primary production: development and skill assessment of regional algorithms. J. Sea Res. 125, 1–17. https://doi.org/10.1016/j.seares.2017.05.004.

Demidov, A.B., Mosharov, S.A., Makkaveev, P.N., 2014. Patterns of the Kara Sea primary production in autumn: biotic and abiotic forcing of subsurface layer. J. Mar. Syst. 132, 130–149. https://doi.org/10.1016/j.jmarsys.2014.01.014.

Erga, S.R., Ssebiyonga, N., Hamre, B., Frette, Q., Hovland, E., Hancke, K., Drinkwater, K., Rey, F., 2014. Environmental control of phytoplankton distribution and photosynthetic performance at the Jan Mayen Front in the Norwegian Sea. J. Mar. Syst. 130, 193205. https://doi.org/10.1016/j.jmarsys.2012.01.006.

Falkowski, P.G., Raven, J.A., 2007. In: Aquatic Photosynthesis, second ed. Princeton University Press, Princeton, NJ, 9780691115511, pp. 488.

Flameling, I.A., Kromkamp, J., 1998. Light dependence of quantum yields for PSII charge separation and oxygen evolution in eucaryotic algae. Limnol. Oceanogr. 43, 284–297.

Garrido, M., Cecchi, P., Vaquer, A., Pasqualini, V., 2013. Effects of sample conservation on assessment of the photosynthetic efficiency of phytoplankton using PAM fluorometry. Deep Sea Res. Part I 71, 38–48. https://doi.org/10.1016/j.dsr.2012.09.004.

Gavrilova, M.K., 1963. Arctic Radiation Climate. Hydrometeorological Publishing House, Leningrad, pp. 224 (in Russian).

Genty, B., Briantais, J.-M., Baker, N.R., 1989. The relationship between the quantum yield of photosynthetic electron transport and quenching of chlorophyll fluorescence. Biochim. Biophys. Acta 990, 87–92.

Glud, R.N., Rysgaard, S., Kühl, M., Hansen, J.W., 2007. The sea ice in Young Sound: implications for carbon cycling. In: In: Rysgaard, S., Glud, R.N. (Eds.), Carbon Cycling in Arctic Marine Ecosystems. Case Study: Young Sound. Medd Grønland. Bioscience 58. The Commission for Scientific Research in Greenland, Copenhagen, pp. 62–85.

Grasshoff, K., Kremling, K., Ehrhardt, M. (Eds.), 1999. Methods of Seawater Analysis, third ed. Wiley-VCH Verlag GmbH, Weinheim, Germany, pp. 577. https://doi.org/10.1002/9783527613984.

Grebecki, A., 1962. Adsorption des fluorochromes par le cystome des Cillies. Bulletin de L'Academie Polonaise des Sciences 10, 483–485.

Hancke, K., Dalsgaard, T., Sejr, M.K., Markager, S., Glud, R.N., 2015. Phytoplankton productivity in an Arctic fjord (West Greenland): estimating electron requirements for carbon fixation and oxygen production. PLoS One 10 (7). https://doi.org/10.1371/journal.pone.0133275. e0133275.

Hancke, K., Hancke, T.B., Olsen, L.M., Johnsen, G., Glud, R.N., 2008. Temperature effects on microalgal photosynthesis-light responses measured by O_2 production, pulse-amplitude-modulated fluorescence, and ^{14}C assimilation. J. Phycol. 44, 501–514 j.1529-8817.2008.00487.x.

Hegseth, E.N., 1997. Phytoplankton of the Barents Sea – the end of a growth season. Polar Biol. 17, 235–241. https://doi.org/10.1007/s003000050127.

Hill, V.J., Cota, G.F., 2005. Spatial patterns of primary production on the shelf, slope and basin of the western arctic in 2002. Deep-Sea Res. Part II 52, 3344–3354. https://doi.org/10.1016/j.dsr2.2005.10.001.

Hobbie, J.E., Daley, R.J., Jasper, S., 1977. Use of nuclepore filters for counting bacteria by fluorescence microscopy. Appl. Environ. Microbiol. 33 (5), 1225–1228. http://aem.asm.org/content/33/5/1225.full.pdf+html.

Holm-Hansen, O., Riemann, B., 1978. Chlorophyll a determination: improvements in methodology. Oikos 30, 438–447. https://doi.org/10.2307/3543338.

Jacques, G., 1983. Some ecophysiological aspects of the Antarctic phytoplankton. Polar Biol. 2, 27–33. https://doi.org/10.1007/BF00258282.

JGOFS (Joint Global Ocean Flux Study Protocols), 1994. Protocols for the Joint Global Ocean Flux Study Protocols (JGOFS) Core Measurements. UNESCO, Paris, pp. 119–122 hdl:10013/epic.27912.d001.

Juneau, P., Harrison, P.J., 2005. Comparison by PAM fluorometry of photosynthetic

activity of nine marine phytoplankton grown under identical conditions. Photochem. Photobiol. 81, 649–653. https://doi.org/10.1111/j.1751-1097.2005.tb00239.x.
Kolber, Z.S., Wyman, K.D., Falkowski, P.G., 1990. Natural variability in photosynthetic energy conversion efficiency: a field study in the Gulf of Maine. Limnol. Oceanogr. 35, 72–79. https://doi.org/10.4319/lo.1990.35.1.0072.
Krause, G.H., Weis, E., 1991. Chlorophyll fluorescence and photosynthesis: the basics. Annu. Rev. Plant Physiol. Plant Mol. Biol. 42, 313–341. https://doi.org/10.1146/annurev.pp.42.060191.001525.
Kromkamp, J.C., Dijkman, N.A., Peene, J., Simis, S.G.H., Gons, H.J., 2008. Estimating phytoplankton primary production in Lake IJsselmeer (The Netherlands) using variable fluorescence (PAM-FRRF) and C uptake techniques. Eur. J. Phycol. 43, 327–344.
Kubryakov, A., Stanichny, S., Zatsepin, A., 2016. River plume dynamics in the Kara Sea from altimetry-based Lagrangian model, satellite salinity and chlorophyll data. Rem. Sens. Environ. 176, 177–187. https://doi.org/10.1016/S0005-2728(98)00135-2.
Lawrenz, E., Silsbe, G., Capuzzo, E., Ylöstalo, P., Forster, R.M., Simis, S.G.H., Prášil, O., Kromkamp, J.C., Hickman, A.E., Moore, C.M., Forget, M.-H., Geider, R.J., Suggett, D.J., 2013. Predicting the electron requirement for carbon fixation in seas and oceans. PLoS One 8 (3). https://doi.org/10.1371/journal.pone.0058137. e58137.
Lippemeier, S., Harting, P., Colijn, F., 1999. Direct impact of silicate on the photosynthetic performance of the diatom *Thalassiosira weissflogii* assessed by on- and off-line PAM fluorescence measurements. J. Plankton Res. 21, 269–283. https://doi.org/10.1093/plankt/21.2.269.
Makarevich, P.R., Larionov, V.V., Moiseev, D.V., 2015. Phytoplankton succession in the Ob-Yenisei shallow zone of the Kara Sea based on Russian databases. J. Sea Res. 101, 31–40. https://doi.org/10.1016/j.seares.2014.10.008.
Manes, S.S., Gradinger, R., 2009. Small scale vertical gradients of Arctic ice algal photophysiological properties. Photosynth. Res. 102, 53–66. https://doi.org/10.1007/s11120-009-9489-0.
Matorin, D.N., Osipov, V.A., Seifullina, N.Kh, Venediktov, P.S., Rubin, A.B., 2009. Increased toxic effect of methylmercury on *Chlorella vulgaris* under high light and cold stress conditions. Microbiology 78 (3), 321–327. https://doi.org/10.1134/S0026261709030102.
Menden-Deuer, S., Lessard, E.J., 2000. Carbon to volume relationships for dinoflagellates, diatoms, and other protist plankton. Limnol. Oceanogr. 45 (3), 569–579. https://doi.org/10.4319/lo.2000.45.3.0569.
Morris, E.P., Kromkamp, J.C., 2003. Influence of temperature on the relationship between oxygen-and fluorescence estimates of photosynthetic parameters in a marine benthic diatom (*Cylindrotheca closterium*). Eur. J. Phycol. 38, 133–142. https://doi.org/10.1080/0967026031000085832.
Mosharov, S.A., 2010. Distribution of the primary production and chlorophyll *a* in the Kara Sea in september of 2007. Oceanology 50 (6), 885–893. https://doi.org/10.1134/S0001437010060081.
Mosharov, S.A., Demidov, A.B., Simakova, U.V., 2016. Peculiarities of the primary production process in the Kara Sea at the end of the vegetation season. Oceanology 56 (1), 84–94. https://doi.org/10.1134/S0001437016010100.
Mosharov, S.A., Sazhin, A.F., Druzhkova, E.I., Khlebopashev, P.V., 2018. Structure and productivity of the phytocenosis in the southwestern Kara Sea in early spring. Oceanology 58 (3), 396–404. https://doi.org/10.1134/S0001437018030141.
Mosharov S.A., Sergeeva V.M., Kremenetskiy V.V., Sazhin A.F., Stepanova S.V., Data Set of Phytoplankton Productive Parameters and Environmental Forces in the Kara Sea in the Autumn. *Data in Brief*, submitted.
Napoleon, C., Raimbault, V., Claquin, P., 2013. Influence of nutrient stress on the relationships between PAM measurements and carbon incorporation in four phytoplankton species. PLoS One 8 (6), e66423. https://doi.org/10.1371/journal.pone.0066423. PMID: 23805221.
Öquist, G.A., Hagstroem, A., Alm, P., Samuelsson, G., Richardson, K., 1982. Chlorophyll-a fluorescence, an alternative method for estimating primary production. Mar. Biol. 68, 71–75. https://doi.org/10.1007/BF00393143.
Platt, T., Harrison, W.G., Horne, E.P.W., Irwin, B., 1987. Carbon fixation and oxygen evolution by phytoplankton in the Canadian High Arctic. Polar Biol. 8, 103–113. https://doi.org/10.1007/BF00297064.
Peterson, T.D., Crawford, D.W., Harrison, P.J., 2011. Mixing and biological production at eddy margins in the eastern Gulf of Alaska. Deep-Sea Res. Part I 58, 377–389. https://doi.org/10.1016/j.dsr.2011.01.010.
Pogosyan, S.I., Galchuk, S.V., Kazimirko, Y.V., 2009. Application of the fluorimeter "MEGA-25" for phytoplankton quantitate and assessment of the photosynthetic apparatus. Water: Chem. Ecol. 6, 34–40 (in Russian).
Ralph, P.J., Gademann, R., Larkun, A., Kuhl, M., 2002. Spatial heterogeneity in active chlorophyll fluorescence and PSII activity of coral tissues. Mar. Biol. 141, 639–646. https://doi.org/10.1007/s00227-002-0866-x.
Röttgers, R., 2007. Comparison of different variable chlorophyll a fluorescence techniques to determine photosynthetic parameters of natural phytoplankton. Deep-Sea Res. Part I 54, 437–451. https://doi.org/10.1016/j.dsr.2006.12.007.
Rudels, B., Jones, E.P., Schauer, U., Eriksson, P., 2004. Atlantic sources of the Arctic Ocean surface and halocline waters. Polar Res. 23 (2), 181–208. https://doi.org/10.1111/j.1751-8369.2004.tb00007.x.
Russo, A.D.P.G., de Souza, M.S., Mendes, C.R.B., Tavano, V.M., Garcia, C.A.E., 2018. Spatial variability of photophysiology and primary production rates of the phytoplankton communities across the western Antarctic Peninsula in late summer 2013. Deep-Sea Res. Part II 149, 99–110.
Sakshaug, E., Bricaud, A., Dandonneau, Y., Falkowski, P.G., Kiefer, D.A., Legendre, L., Morel, A., Parslow, J., Takahashi, M., 1997. Parameters of photosynthesis: definitions, theory and interpretation of results. J. Plankton Res. 19, 1637–1670. https://doi.org/10.1093/plankt/19.11.1637.
Sazhin, A.F., Artigas, L.F., Nejstgaard, J.C., Frischer, M.E., 2007. The colonization of two *Phaeocystis* species (Prymnesiophyceae) by pennate diatoms and other protists: a significant contribution to colony biomass. Biogeochemistry 83, 137–145. https://doi.org/10.1007/s10533-007-9086-2.
Schloss, I.R., Ferreyra, G.A., 2002. Primary production, light and vertical mixing in Potter Cove, a shallow bay in the maritime Antarctic. Polar Biol. 25, 41–48. https://doi.org/10.1007/s003000100309.
Schreiber, U., 1998. Chlorophyll fluorescence: new instruments for special applications. In: In: Garab, G. (Ed.), Photosynthesis: Mechanisms and Effects V. Kluwer Academic Publishers, Dordrecht, pp. 4253–4258.
Schreiber, U., 2004. Pulse amplitude (PAM) fluorometry and saturation pulse method: an overview. In: Papageorgiou, G., Govindjee, G. (Eds.), Chlorophyll *a* Fluorescence: a Signature of Photosynthesis. Advances in Photosynthesis and Respiration Series. Kluwer Academic Publishers, Dordrecht, pp. 270–319.
Schreiber, U., Bilger, W., Neubauer, C., 1994. Chlorophyll fluorescence as a non intrusive indicator for rapid assessment of in vivo photosynthesis. In: Schulze, E., Caldwell, M. (Eds.), Ecophysiology of Photosynthesis. Springer-Verlag, Berlin, pp. 49–70.
Sergeeva, V.M., Sukhanova, I.N., Mosharov, S.A., Kremenetskiy, V.V., Poluhin, A.A., Druzhkova, E.I., 2016. The structure and distribution of the phytoplankton community in the deep region of the Northern Kara Sea. Oceanology 56 (1), 107–113. https://doi.org/10.1134/S0001437016010197.
Steemann-Nielsen, E., 1952. The use of radio-active carbon (C14) for measuring organic production in the sea. Journal du Conseil/Conseil Permanent International pour l'Exploration de la Mer 18, 117–140. https://doi.org/10.1093/icesjms/18.2.117.
Strickland, J.D.H., Parsons, T.R., 1972. In: A Practical Handbook of Seawater Analysis, second ed. Fisheries Research Board of Canada, Ottawa, pp. 310.
Suggett, D.J., MacIntyre, H.L., Kana, T.M., Geider, R.J., 2009a. Comparing electron transport with gas exchange: parameterising exchange rates between alternative photosynthetic currencies for eukaryotic phytoplankton. Aquat. Microb. Ecol. 56, 147–162. https://doi.org/10.3354/ame01303.
Suggett, D.J., Moore, C.M., Hickman, A.E., Geider, R.J., 2009b. Interpretation of fast repetition rate (FRR) fluorescence: signatures of phytoplankton community structure versus physiological state. Mar. Ecol. Prog. Ser. 376, 1–19. https://doi.org/10.3354/MEPS07830.
Suggett, D.J., Prasil, O., Borowitzka, M.A. (Eds.), 2010. Chlorophyll a Fluorescence in Aquatic Sciences: Methods and Applications. Developments in Applied Phycology 4 Springer Science + Business Media. https://doi.org/10.1007/978-90-481-9268-7_6.
Sukhanova, I.N., 1983. Concentration of phytoplankton in a sample. In: Vinogradov, M.E. (Ed.), Modern Techniques of Quantitative Assessment of Sea Plankton Distribution. Nauka, Moscow, pp. 97–105 (in Russian).
Sukhanova, I.N., Flint, M.V., Mosharov, S.A., Sergeeva, V.M., 2010. Structure of the phytoplankton communities and primary production in the Ob River estuary and over the adjacent Kara Sea shelf. Oceanology 50 (5), 743–758. https://doi.org/10.1134/S0001437010050115.
Sukhanova, I.N., Flint, M.V., Sazhin, A.F., Sergeeva, V.M., Druzhkova, E.I., 2015a. Phytoplankton in the northwestern Kara Sea. Oceanology 55 (4), 547–560. https://doi.org/10.1134/S0001437015040141.
Sukhanova, I.N., Flint, M.V., Sergeeva, V.M., Nedospasov, A.A., Druzhkova, E.I., 2015b. Structure of phytoplankton communities in the Yenisei estuary and over the adjacent Kara Sea shelf. Oceanology 55 (6), 844–857. https://doi.org/10.1134/S0001437015060193.
Sun, J., Liu, D., 2003. Geometric models for calculating cell biovolume and surface area for phytoplankton. J. Plankton Res. 25 (11), 1331–1346. https://doi.org/10.1093/plankt/fbg096.
Throndsen, J., Hasle, G.R., Tangen, K., 2007. Phytoplankton of Norwegian Coastal Waters. Almater Foprlag AS, Oslo, pp. 341 ISBN-13: 9788278580868.
Tomas, C.R. (Ed.), 1997. Identifying Marine Phytoplankton. Academic Press, San Diego, CA, pp. 858. https://doi.org/10.1017/S0025315400038959.
Tripathy, S.C., Pavithran, S., Sabu, P., Pillai, H.U.K., Dessai, D.R.G., Anilkumar, N., 2015. Deep chlorophyll maximum and primary productivity in Indian Ocean sector of the Southern Ocean: case study in the Subtropical and Polar Front during austral summer 2011. Deep-Sea Res. Part II 118, 240–249. https://doi.org/10.1016/j.dsr2.2015.01.004.
Yun, M.S., Chung, K.H., Zimmermann, S., Zhao, J., Joo, H.M., Lee, S.H., 2012. Phytoplankton productivity and its response to higher light levels in the Canada Basin. Polar Biol. 35, 257–268. https://doi.org/10.1007/s00300-011-1070-6.
Zatsepin, A.G., Morozov, E.G., Demidov, A.N., Kremenetskiy, V.V., Poyarkov, S.G., Paka, V.T., Kondrashov, A.A., Korzh, A.O., Soloviev, D.M., 2010b. Circulation in the southwestern part of the Kara Sea in september 2007. Oceanology 50 (5), 643–656. https://doi.org/10.1134/S0001437010050024.
Zatsepin, A.G., Poyarkov, S.G., Kremenetskiy, V.V., Nedospasov, A.A., Shchuka, S.A., Baranov, V.I., Kondrashov, A.A., Korzh, A.O., 2015. Hydrophysical features of deep water troughs in the western Kara Sea. Oceanology 55 (4), 472–484. https://doi.org/10.1134/S0001437015040165.
Zatsepin, A.G., Zavialov, P.O., Kremenetskiy, V.V., Poyarkov, S.G., Soloviev, D.M., 2010a. The upper desalinated layer in the Kara Sea. Oceanology 50 (5), 658–668. https://doi.org/10.1134/S0001437010050036.